

Microscopic analysis of the coherent optical generation and the decay of charge and spin currents in semiconductor heterostructures

Huynh Thanh Duc, T. Meier, and S. W. Koch
 Department of Physics and Material Sciences Center,
 Philipps University, Renthof 5, D-35032 Marburg, Germany
 (Dated: April 14, 2024)

The coherent optical injection and temporal decay of spin and charge currents in semiconductor heterostructures is described microscopically, including excitonic effects, carrier LO-phonon and carrier-carrier scattering, as well as nonperturbative light-field-induced intraband and interband excitations. A nonmonotonous dependence of the currents on the intensities of the laser beams is predicted. Enhanced damping of the spin current relative to the charge current is obtained as a consequence of spin-dependent Coulomb scattering.

PACS numbers: 72.25.Fe, 42.65.-k, 72.25.Rb

One of the fundamental principles of quantum mechanics is that superpositions of wave functions lead to interference phenomena which depend on the relative phase differences. In the coherent regime, e.g., shortly after an external perturbation has generated a nonequilibrium situation, such quantum mechanical interference effects can be employed for the coherent control of dynamical processes in atomic, molecular, biological, and semiconductor systems [1, 2, 3, 4, 5, 6]. Many of the measurements and proposals in this area make use of the coherent evolution of electronic excitations induced by specially designed optical laser pulses, e.g., sequences of phase-locked or suitably chirped beams.

In semiconductors, the ultrafast coherent generation of photocurrents using two light beams with frequencies ω_1 and ω_2 has attracted considerable attention [7, 8, 9]. As shown in Ref. 10, the same type of interference scheme can also be employed to create pure spin currents which are not accompanied by any charge current. Such spin currents generated on ultrafast time scales have been observed in semiconductors [11, 12] and could be useful for future applications in the area of spintronics [13, 14]. As shown recently, it is even possible to control photocurrents via the carrier-envelope phase [15, 16] which makes this scheme also interesting for optical metrology. Furthermore, for disordered semiconductors it has been predicted that sequences of temporally delayed excitation pulses can be used to induce current echoes [17].

The coherent generation of photocurrents in semiconductors by two light fields with frequencies ω_1 and ω_2 satisfying $2\hbar\omega_1 > E_{\text{gap}} > \hbar\omega_2$, where E_{gap} is the band gap energy, has first been described in terms of nonlinear optical susceptibilities which have been obtained on the basis of band structure calculations [8, 18]. In this framework, the optically-induced intra- and interband transitions are treated within Fermi's golden rule. The interference between intra- and interband excitations leads to electron and hole distributions which are not symmetric in k -space corresponding to a nonequilibrium situation with a finite current. The dynamics of the generation

process has been analyzed using Bloch equations. This approach has been applied to disordered semiconductors within a two-band model [17] and to ordered quantum wells within a multiband formalism [19]. Although the relaxation of the photocurrent by carrier LO-phonon scattering in bulk GaAs has been analyzed [20], in most of the existing publications the temporal decay of the charge and spin currents is still modeled by phenomenological decay times [11, 12, 15, 16]. The Coulomb interaction among the photoexcited carriers has so far not been the focus of particular attention. However, excitonic effects in quantum wires have recently been addressed on the Hartree-Fock level [21].

In this letter, we present and analyze a microscopic many-body theory that is capable of describing the dynamical generation, the coherent evolution, and the decay of charge and spin currents. Our approach is based on the semiconductor Bloch equations (SBE), i.e., the equations of motion for the optical polarization and the carrier populations [22, 23]. The equations nonperturbatively include the light-field-induced intraband and interband excitations without a rotating wave approximation. The approach is thus capable of describing the nontrivial dependence of the initially generated currents on the intensities of the incident fields beyond the perturbative regime. The coherent part of the SBE contains the Coulomb interaction among the photoexcited carriers on the Hartree-Fock level, i.e., excitonic effects and Coulomb-bic nonlinearities due to energy and field renormalizations. As correlation contributions we include carrier-LO-phonon and carrier-carrier scattering at the second Born-Markov level [22, 23].

The dynamical optoelectronic response is analyzed using the Heisenberg equations of motion for the carrier populations $n_k^e = \langle a_{c,k}^\dagger a_{c,k} \rangle$ and $n_k^h = 1 - \langle a_{v,k}^\dagger a_{v,k} \rangle$ and the interband polarization $p_k = \langle a_{v,k}^\dagger a_{c,k} \rangle$. Here, $a_{v,k}^\dagger$ ($a_{c,k}$) creates (destroys) an electron with wave vector k and spin in band v (c). The resulting SBE including

intra- and interband excitations read [24, 25]

$$\begin{aligned} \left(\frac{d}{dt} + \frac{e}{h} E(t) \right) r_k p_k &= \frac{d}{dt} p_k^{\text{coll}} \\ \frac{i}{h} [c_k - v_k] \sum_{q \neq 0} V_q (n_{k+q}^e + n_{k+q}^h) p_k & \\ \frac{i}{h} (n_k^e + n_k^h - 1) (d_{k}^{\text{cv}} E(t) + \sum_{q \neq 0} V_q p_{k+q}) & \end{aligned} \quad (1)$$

$$\begin{aligned} \left(\frac{d}{dt} + \frac{e}{h} E(t) \right) r_k n_k &= \frac{d}{dt} n_k^{\text{coll}} \\ \frac{2}{h} \text{Im} [(d_{k}^{\text{cv}} E(t) + \sum_{q \neq 0} V_q p_{k+q}) p_k] & \end{aligned} \quad (2)$$

where $r_k = e/h$, V_q denotes the Coulomb interaction potential, and d_k^{cv} is the interband transition dipole. The terms given explicitly in Eqs. (1)–(2) describe the dynamics on the time-dependent Hartree-Fock level. The incoherent contributions are denoted by j_{coll} . Here, these collision terms describe carrier LO-phonon and carrier-carrier scattering in the second-order Born-Markov approximation [22, 23].

Except for the explicit inclusion of the spin, equations similar to Eqs. (1)–(2) have been used to describe the optoelectronic response of semiconductor superlattices in the presence of static and Terahertz elds [24, 25]. In these studies, the optical elds have been considered to generate interband transitions via $E(t) d_k^{\text{cv}}$ and the static and Terahertz elds lead to the intraband acceleration via $E(t) r_k$. This distinction is useful if the involved elds are characterized by very different frequencies. However, since we here describe the generation of currents by the interference of optical elds with frequencies ω_1 and ω_2 , this simplification is not possible and thus the total eld is considered for both the intra- and interband excitations.

Numerical solutions of Eqs. (1)–(2) provide the time-dependent polarization and populations. The populations in the valence and conduction bands determine the charge and spin current densities which are given by $J = e \sum_k p_k v_k n_k^e - e \sum_k v_k n_k^h$ and $S = \frac{\hbar}{2} \sum_k v_k n_k^e - \frac{\hbar}{2} \sum_k v_k n_k^h$, respectively, where $v = r_k \hbar$ is the group velocity.

The coherent generation of currents is due to material excitations which are not symmetric in k -space. In such situations, solutions of Eqs. (1)–(2) including the scattering contributions are quite demanding. In order to keep the numerical requirements within reasonable limits we consider for the present analysis two model systems: a one-dimensional (1D) quantum wire and a two-dimensional (2D) quantum well representative of a GaAs/AlGaAs system. The electronic band structure is described in effective mass approximation using $m_c = 0.067 m_0$ and $m_v = 0.457 m_0$, and the band gap is $E_{\text{gap}} = 1.5$ eV. The interband transition dipoles are

taken as $d_k^{\text{cv}} = d_{\text{cv}}(1; i; 0)$ and $d_{\#k}^{\text{cv}} = d_{\text{cv}}(1; -i; 0)$ with $d_{\text{cv}} = 3 eA$, i.e., we use the usual circularly polarized dipole matrix elements which describe heavy hole to conduction band transitions in quantum wells close to the Γ -point [26]. The incident laser eld is given by

$$E(t) = \sum_{\omega_1, \omega_2} e A (e^{i(\omega_1 t - \phi_1)} + e^{i(\omega_2 t - \phi_2)} + \text{c.c.}); \quad (3)$$

where e denotes the polarization, A the amplitude, and ϕ_1, ϕ_2 the phase of the eld of frequency ω_1 and ω_2 , respectively. Both frequency components are Gaussian shaped pulses with a duration determined by τ_L . For the case that both eld components are linearly polarized in x -direction, i.e., $e_1 = e_2 = e_x$ the photoexcitation produces a pure charge current since the two spin systems are excited identically. For the case of linear perpendicularly polarized pulses, i.e., $e_1 = e_x$ and $e_2 = e_y$, a pure spin current with no accompanying charge current is generated. Since the charge (spin) current is proportional to $\sin(\omega_2 - \omega_1)$ [$\cos(\omega_2 - \omega_1)$] [10] we use $\omega_2 - \omega_1 = \omega$ ($\omega_2 + \omega_1 = \omega$) in our calculations to obtain maximal currents.

Time-dependent electron and hole distributions of a quantum well in k -space are shown in Fig. 1. The carriers are initially generated with a combined excess energy of 150 meV above the band gap. Due to their smaller mass about 130 meV of the kinetic energy is given to the electrons and the excess energy of the holes is only about 20 meV. Therefore, the electron relaxation is considerably influenced by LO-phonon emission whereas the hole distribution is only weakly affected. Immediately after the excitation, the electron and hole distributions are very similar, see Fig. 1. Both are generated nonuniformly on a ring with radius $r_0 = a_0$. Due to the quantum interference, the distributions are larger for positive k_x than for negative k_x . Thus the distributions have a nonvanishing positive average momentum which corresponds to a current in x -direction. In the course of time, the distributions relax towards quasi-equilibrium distributions. For long times, due to their larger mass the distribution of the holes is wider than that of the electrons.

Figure 2(a) demonstrates that for the considered excitation conditions both carrier LO-phonon and carrier-carrier scattering contribute significantly to the current dynamics. If only carrier LO-phonon scattering is taken into account, the charge and spin currents decay similarly. This decay is not exponential, however, its onset can be described by an exponential decay with time constant 240 fs. When carrier-carrier scattering is included, the currents decay more rapidly and, in particular, the spin current decays faster than the charge current. Additional calculations which omit specific contributions have revealed that this difference is due to Coulomb scattering between carriers with different spin. When a charge current is excited ($e_1 = e_2 = e_x$), the electron distributions for different spin are equal $n_k^e = n_{\#k}^e$. Thus,

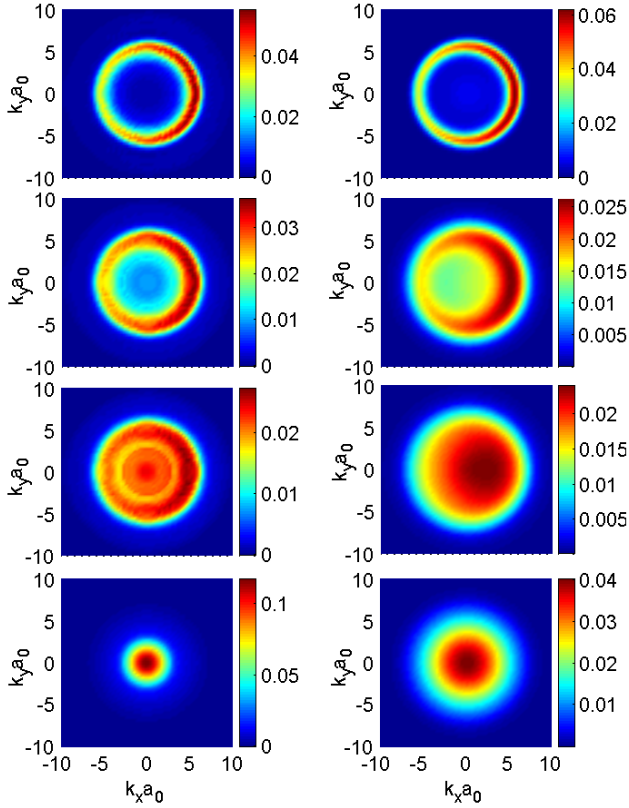


FIG. 1: (color) Left (right) column: Contour plots of the electron (hole) distributions of a quantum well in k -space at $t = 50, 100, 150$, and 400 fs (from top to bottom), respectively. The incident pulses have a duration of $\tau_L = 20$ fs, the amplitudes are $A_1 = 2A_{21} = 108A_0$, with $A_0 = E_0 = ea_0/4 \cdot 10^3$ V/cm, where E_0 is the three-dimensional exciton Rydberg, and $2\hbar = 1.65$ eV. The density of the photojected carriers is $N = 10^{11}$ cm $^{-2}$ and the temperature is $T = 50$ K. a_0 is the three-dimensional exciton Bohr radius.

in this case both spins have the same nonvanishing average momentum. Since carrier-carrier scattering only exchanges momentum among the carriers, this average momentum is not reduced by the Coulomb scattering. The situation is, however, different when a spin current is excited ($e_1 = e_x, e_2 = e_y$). In this case the electron distributions satisfy $n_{\mathbf{k}}^e = n_{-\mathbf{k}}^e$ where \mathbf{k} has the same y -component as \mathbf{k} but its negative x -component, i.e., the average momenta of the two spins point into opposite directions. Therefore, the total electron momentum vanishes and Coulomb scattering leads to a decay of the average momenta of the spin-up and spin-down electrons. Fig. 2(b) shows that qualitatively similar results are obtained for quantum wires. However, due to the smaller 1D phase space, the scattering is reduced and thus the decay times are longer than in 2D. The results presented in Fig. 2 and of additional evaluations show that i) at low densities the charge and spin currents decay with the same time constant due to carrier LO-phonon scattering and ii) with increasing density, carrier-carrier scattering

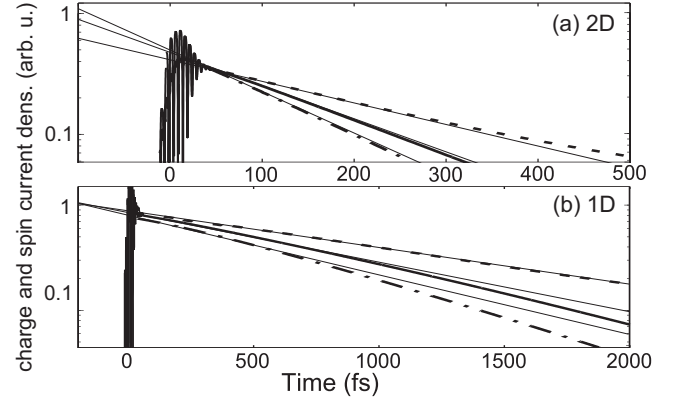


FIG. 2: (a) Time-dependent charge (solid) and spin (dash-dot) currents of a quantum well for the same parameters as in Fig. 1. Also shown is the identical decay of both currents if only carrier LO-phonon scattering is considered (dashed). The thin solid lines represent exponential decays with time constants of 240, 155, and 125 fs, respectively. (b) Same as (a) for a quantum wire. The density of the photojected carriers is $N = 5 \cdot 10^5$ cm $^{-1}$ and the other parameters are the same as in (a). The thin solid lines represent exponential decays with time constants of $\tau = 1250, 900$, and 740 fs, respectively.

speeds up the decay of both currents, however, the rate of change is larger for the spin than for the charge current.

Since 2D calculations are numerically extensive, we present in the following results obtained in 1D. Qualitatively similar effects should also be present in 2D. Fig. 3(a) shows how the injected carrier density depends on the field amplitude $A = A_{21} = A_1/2$. In the considered regime, the density increases approximately linear with A . However, the current depends on A in a strongly nonlinear fashion, see Fig. 3(b). For small amplitudes, the nonsymmetric k -space carrier distributions increase with A without significant distortion. Therefore, in this regime both the total density and the charge current become larger with increasing A . At a certain excitation level the peak of the generated distribution becomes comparable to 1 and further excitation is reduced by the Pauli principle. Thus, in the high-field regime the asymmetry of the k -space distribution and the current decrease with increasing field amplitude.

Figures 3(c) and (d) show how the carrier and the charge current densities depend on the ratio of the field amplitudes $x = A_1/A_{21}$ for a fixed amplitude of the 21 field $A_{21} = 128A_0$. At $x = 0$, only the 21 field is present which generates via interband excitations symmetric carrier distributions in k -space, i.e., no current. A finite current is present only if x is finite since the combined action of inter- and intraband excitations is required for the generation of nonsymmetric k -space carrier distributions. In the limit of small x the current increases as x^2 in agreement with a perturbative analysis of the light-matter coupling. In this regime, the carrier density increases only slightly with x since a weak 1 field

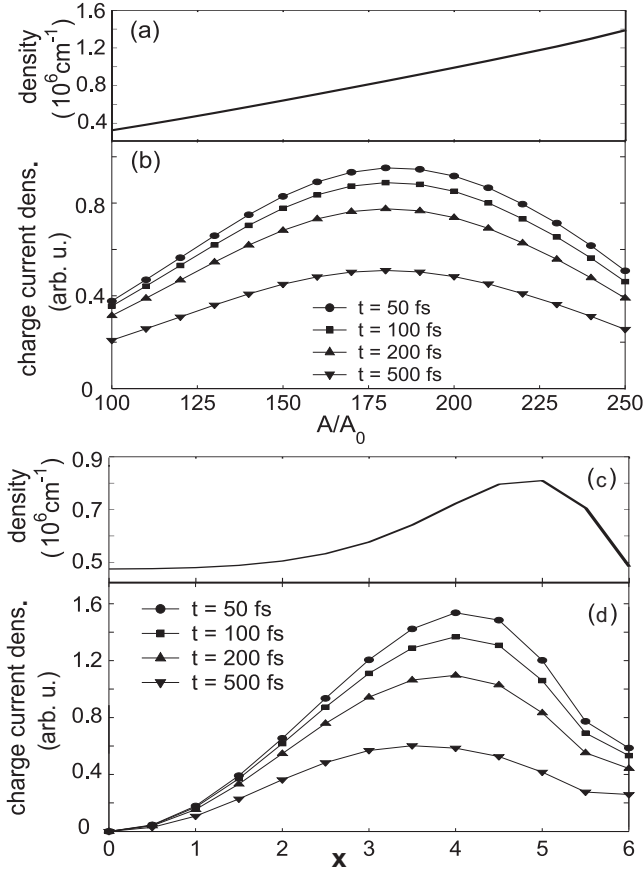


FIG. 3: Dependence of (a) the carrier density and (b) the charge current density at different times on the amplitude $A = A_2! = A_1! = 2$ of the incident pulses in a quantum wire. Dependence of (c) the carrier density and (d) the charge current density on the amplitude ratio $x = A_1! = A_2!$ for $A_2! = 128A_0$. Here, we use $2\hbar! = 1.62 \text{ eV}$ and $T = 50 \text{ K}$.

predominantly redistributes the carriers in k -space by introducing asymmetries. Beyond this perturbative regime we find an interesting dependence of both the carrier density and the current on x . The largest current is obtained for $x \approx 4$, i.e., $A_1! \approx 512A_0$. It can be expected that for optical frequencies, the x which generates the largest current is always larger than 1, since intraband excitations are relatively smaller than interband excitations. We find that the optimal value of x increases with decreasing $A_2!$. Thus in the limit of weak fields $A_1!$ should be chosen much larger than $A_2!$ if one is interested in generating large currents. Our calculations have shown that the intensity dependence of the spin current is very similar that of the charge current, see Fig. 3.

In summary, the coherent optical injection and the decay of charge and spin currents in semiconductor heterostructures is described by a microscopic many-body theory. We find that due to Coulomb scattering between carriers of different spin at elevated excitation levels the spin current decays more rapidly than the charge cur-

rent. An interesting nonmonotonous dependence of the currents on the intensities of the laser beams is predicted. These results should stimulate further experimental research in this direction.

This work is supported by the Deutsche Forschungsgemeinschaft (DFG), by the Ministry of Education and Research (BMF), and by the Center for Optodynamics, Philipps University, Marburg, Germany. We thank the John von Neumann Institut für Computing (NIC), Forschungszentrum Jülich, Germany, for grants for extended CPU time on their supercomputer systems.

-
- [1] P. Bruner and M. Shapiro, Chem. Phys. Lett. 126, 541 (1986).
 - [2] W. S. Warren, H. Rabitz, and M. Dahlem, Science 259, 1581 (1993).
 - [3] R. J. Gordon and S. A. Rice, Ann. Rev. Phys. Chem. 48, 601 (1997).
 - [4] T. Brabec and F. Krausz, Rev. Mod. Phys. 72, 545 (2000).
 - [5] J. L. Herek et al., Nature 417, 533 (2002).
 - [6] M. Shapiro and P. Bruner, Rep. Prog. Phys. 66, 859 (2003).
 - [7] E. Dupont et al., Phys. Rev. Lett. 74, 3596 (1995).
 - [8] R. Atanasov et al., Phys. Rev. Lett. 76, 1703 (1996).
 - [9] A. Hache et al., Phys. Rev. Lett. 78, 306 (1997).
 - [10] R. D. R. Bhat and J. E. Sipe, Phys. Rev. Lett. 85, 5432 (2000).
 - [11] M. J. Stevens et al., Phys. Rev. Lett. 90, 136603 (2003).
 - [12] J. Hubner et al., Phys. Rev. Lett. 90, 216601 (2003).
 - [13] S. A. Wolf et al., Science 294, 1488 (2001).
 - [14] I. Zutic, J. Fabian, and S. Das Sarma, Rev. Mod. Phys. 76, 323 (2004).
 - [15] T. M. Fortier et al., Phys. Rev. Lett. 92, 147403 (2004).
 - [16] P. A. Ross et al., J. Opt. Soc. Am. B 22, 362 (2005).
 - [17] C. Schlichenmaier et al., Phys. Rev. B 65, 085306 (2002).
 - [18] A. Najmaie, R. D. R. Bhat, and J. E. Sipe, Phys. Rev. B 68, 165348 (2003).
 - [19] D. H. M. arti, M. A. Dupont, and B. Deveaud, Phys. Rev. B 69, 035335 (2004).
 - [20] P. Kral and J. E. Sipe, Phys. Rev. B 61, 5381 (2000).
 - [21] D. H. M. arti, Ph.D. thesis, Ecole Polytechnique Fédérale de Lausanne, Switzerland, 2003.
 - [22] H. Haug and S. W. Koch, Quantum Theory of the Optical and Electronic Properties of Semiconductors, 4th ed. (World Scientific, Singapore, 2004).
 - [23] W. Schafer and M. Wegener, Semiconductor Optics and Transport Phenomena, (Springer, Berlin, 2002).
 - [24] T. Meier et al., Phys. Rev. Lett. 73, 902, (1994).
 - [25] T. Meier et al., Phys. Rev. Lett. 75, 2558 (1995).
 - [26] These matrix elements are clearly not realistic for quantum wires. This model, however, allows us to perform detailed investigations of the currents in a 1D system with rather modest numerical requirements. The obtained results are useful since the fundamental dependencies and the differences between the decay of the charge and spin currents are similar in 2D.